Dalton Transactions

Accepted Manuscript

This is an *Accepted Manuscript*, which has been through the Royal Society of Chemistry peer review process and has been accepted for publication.

Accepted Manuscripts are published online shortly after acceptance, before technical editing, formatting and proof reading. Using this free service, authors can make their results available to the community, in citable form, before we publish the edited article. We will replace this *Accepted Manuscript* with the edited and formatted *Advance Article* as soon as it is available.

You can find more information about *Accepted Manuscripts* in the Information for Authors.

Please note that technical editing may introduce minor changes to the text and/or graphics, which may alter content. The journal's standard Terms & Conditions and the Ethical guidelines still apply. In no event shall the Royal Society of Chemistry be held responsible for any errors or omissions in this *Accepted Manuscript* or any consequences arising from the use of any information it contains.

ROYAL SOCIETY OF CHEMISTRY

www.rsc.org/dalton

Cite this: DOI: 10.1039/c0xx00000x

www.rsc.org/xxxxxx

PAPER

Influence of reduction temperature on composition, particle size, and magnetic properties of CoFe alloy nanomaterials derived from layered double hydroxides precursors

Shuangxia Yang,[a] Lianying Wang,*[a] Shuang Yue,[a] Yanluo Lu,[a] Jing He[a] and Dongye Zhao[b]

Received (in XXX, XXX) Xth XXXXXXXXX 20XX, Accepted Xth XXXXXXXXX 20XX
DOI: 10.1039/b000000x

Individual CoFe alloy nanoparticles and CoFe-MgO nanocomposites were prepared through thermal reduction of single-source layered double hydroxides (LDHs) precursors at various temperatures. The samples were characterized by X-ray diffraction (XRD), scanning electron microscope (SEM), transmission electron microscopy (TEM), and vibrating sample magnetometer (VSM) analyses to investigate the influence of reduction temperature on the composition, particle size and size distribution, as well as the magnetic properties of the resulting materials. XRD and SEM results show that the as-prepared CoFe alloy nanoparticles and CoFe-MgO nanocomposites display high crystallinity and high purity. The average particle size of individual CoFe nanoparticles increases with the increase of reduction temperature. In the presence of MgO matrix, uniform CoFe alloy nanoparticles with a narrow diameter distribution (8-11 nm) were obtained. Magnetic measurement indicates that the saturation magnetization strength (Ms) of the resulting materials increases with reduction temperature. The individual CoFe alloy nanoparticles exhibit excellent soft magnetic behavior with an extremely high Ms value (213 emu/g at 800 ^{o}C), comparable to that of bulk CoFe alloy (230 emu/g). For CoFe-MgO nanocomposites, small Ms values were obtained due to the small CoFe alloy particle size and low percentage of magnetic component. However, the coercivities are greatly enhanced (663 Oe at 450 ^{o}C) for the composites, implying their potential applications in data storage and other magnetic devices.

Introduction

Over the past decade, research activity in the field of metal nanoparticles has grown dramatically. Numerous alloy nanoparticles, such as AuAg, NiM or FeM (where M=Pt, Sn, Pd and Co) have been investigated for their fundamental importance as well as their technological applications.[1] As an important transition metal alloy, CoFe alloy shows extraordinary mechanical, electrical, catalytic and magnetic properties, which are very interesting for technical applications, e.g., in biotechnology,[2a] catalysis[2b] and electronic devices.[2c] Eespecially, CoFe alloy is an important soft magnetic material with high saturation magnetizations (upto 2.45 T), high resistivity, small coercive forces, high curie temperature, and high magnetic anisotropy energies, which make them potential candidates for ultra-high-density magnetic recording media and many other areas.[3] Most of the applications require chemically stable nanoparticles having definite composition, uniform size and shape; in the case of bimetallic nanoparticles, this is particularly difficult to achieve.[4] Many groups have devoted their attentions to the synthesis of alloy nanomaterials with controllable morphology, composition, and particle size, which are primary variables determining physical (such as magnetic, optical, etc.) as well as chemical (reactivity, catalysis, etc.) properties of materials. For example, Mandal et al. have synthesized sphere- and rod-shaped superparamagnetic NiPt alloy by solution-phase wet chemical reduction of mixted metal ions precursors with the surfactant CTAB as a stabilizing agent.[5a] Wang and co-workers reported the synthesis of CoFe alloyed nanoparticles consisting of metallic cores and oxide shells by chemical vapor condensation using a mixture of organomatellic iron carbonyl and cobalt carbonyl as precursors.[5b] Song and co-workers have prepared FePt nanocrystals with controllable stoichiometry by using a single bimetallic compound precursor.[5c] Moreover, the unique physical and chemical properties of the alloy nanomaterials depend not only on the characteristics of individual nanoparticles, but also on their coupling and interaction, which can be tuned by the uniform dispersion of the particles in an organic/inorganic matrix. Therefore, various nanocomposites consisting of alloy nanoparticles embedded in a insulating matrix have been widely investigated. For example, Ennas and co-workers[6, 4b] did many studies in the preparation of CoFe alloy nanocomposites with alloy nanoparticles uniformly dispersed in different matrixs (SiO_2, Al_2O_3) via a sol-gel process and the influence of composition or preparation conditions on the structure and magnetic properties of the resulting composites. Manners et al.[7] have synthesized magnetic CoFe alloy nanoparticle-containing ceramics material with controllable alloy composition and particle size by pyrolysis of highly metallized polymer precursors. However, most of the

Dalton Transactions Accepted Manuscript

techniques mentioned above are based on mixture of precursors or organometallic precursors, which have limitations in control over the purity and composition of the resulting alloy materials or involve environmentally unfriendly and expensive complex chemicals.

By virtue of their tunable composition, uniform distribution of cations on the layer, ease of preparation, low-cost, as well as environmentally green property, layered double hydroxides (LDHs) are well known precursors for preparing well dispersed metal and multi-metal oxide nanoparticles with controllable composition and particle size, which are widely used as magnetic materials,[8a] catalyst-supports,[8b] and catalysts.[8c] In our previous work, CoFe alloy nanoparticles uniformly embedded in a MgO crystal matrix with tuable composition were synthesized by thermal reduction of a single-source MgCoFe-CO_3-LDHs precursor.[9] In this work, we aimed to further investigate the influence of reduction temperature on the composition, morphology, particle size, and magnetic properties of the CoFe-MgO nanocomposites. Individual CoFe alloy nanoparticles were prepared and studied together, which in itself is of interest since this material has not been synthesized by such a facile, green, and low-cost method. Furthermore, the MgO matrix is expected to influence not only the formation and growth of the dispersed CoFe alloy nanoparticles, but also the resulting magnetic properties of the nanocomposites.

Experimental Section

Synthesis of CoFe-LDHs and MgCoFe-LDHs Precursors

All chemicals were used as received without further purification. The uniform CoFe-LDHs precursor with interlayer CO_3^{2-} anions was prepared by a procedure involving separated nucleation and aging steps (SNAS method).[10] A mixture of $Co(NO_3)_26{\cdot}H_2O$ and $Fe(NO_3)_3{\cdot}9H_2O$ with Co/Fe molar ratio of 2/1 was dissolved in 100 mL of deionized water to form a clear solution ($[Co^{2+}] + [Fe^{3+}]$) = 1.0 M). The mixed salt solution and 100 mL of another Na_2CO_3 and NaOH mixed aqueous solution ($[OH^-]$ = 1.6 M, $[CO_3^{2-}] = 2[Fe^{3+}]$) were simultaneously added to a colloid mill with rotor speed of 3000 rpm and mixed for 1 min. The resulting suspension was transferred into a Teflon-lined autoclave and crystallized at 100 °C for 24 h. The resulting solid product was separated by centrifugation, washed with deionized water several times until pH = 7, and dried in an oven at 60 °C for 12 h to collect the solid powder CoFe LDHs product. The MgCoFe-LDHs precursor with interlayer CO_3^{2-} anions was prepared through the same process, of which the compositions were fixed as n(Mg)/n(Co)/n(Fe)= 3.5/1.5/1.

Synthesis of CoFe alloy and CoFe-MgO nanocomposites

The CoFe alloy particles and CoFe-MgO nanocomposites were prepared by reduction of as-synthesized CoFe-LDHs and MgCoFe-LDHs precursors. In a typical process, the LDHs precursors were placed in a ceramic boat which was placed in a furnace and purged with a mixed gas (5% H_2+95% N_2) for 2 min to exclude the oxygen in the furnace. Under continuous flow (60 mL/min) of N_2/H_2 gas, the furnace temperature was raised at a ramping rate of 5 °C/min and then kept at 450 °C, 600 °C, 700 °C, and 800 °C for 2 h, respectively. Then the furnace was slowly cooled down naturally to room temperature.

Characterization

X-ray diffraction (XRD) patterns of the samples were recorded using a Shimadzu XRD-6000 diffractometer under the following conditions: 40 kV, 30 mA, Cu $K_{\alpha1}$ radiation (λ = 0.15406 nm). The samples were step-scanned in steps of 10 °/min in the 2θ range from 3° to 90°.

Fourier transform infrared (FT-IR) spectra were recorded in the range 4000 cm^{-1} to 400 cm^{-1} with 2 cm^{-1} resolution on a Bruker Vector-22 Fourier transform spectrometer using the KBr pellet technique (1 mg of sample in 100 mg of KBr).

Thermogravimetric and differential thermal analysis (TG-DTA) were carried out on a HCT-2 thermal analysis system produced locally. Samples of 10.0 mg were heated at a rate of 10 °C/min with an N_2 flow rate of 40 cm^3 /min^{-1} up to 900 °C.

Temperature-programmed reduction (TPR) analysis was carried out in a Micromeritics TPR/TPD 2900 instrument at a heating rate of 10 °C min^{-1} and using a H_2/Ar (10% vol) mixture gases as reducing agent (60 mL min^{-1}). The temperature was raised from 30 to 900 °C and then cooled to ambient temperature. Experimental conditions for TPR runs were chosen according to datas reported elsewhere[11] in order to attain good resolution of component peaks and the calibration was carried out from reduction of CuO (from Merck).

Scanning electron microscope (SEM) images were obtained using a Hitachi S-4700 field emission SEM at 10 kV, combined with energy dispersive X-ray spectroscopy (EDX) for the determination of metal compositions. The surface of the sample was coated with a thin platinum layer to avoid a charging effect.

Transmission electron microscopy (TEM) was performed on a Hitachi H-800 microscope with an accelerating voltage of 200 kV. The sample was ultrasonically dispersed in an appropriate amount of ethanol and a drop of the resulting suspension was deposited on a carbon-coated Cu grid followed by evaporation of the solvent in air.

Magnetic properties of samples were measured at room temperature on a locally made JDM-13 vibrating sample magnetometer. The mass of the sample was 20 mg.

Results and discussion

Synthesis and Characterization of CoFe-LDHs and MgCoFe-LDHs precursors

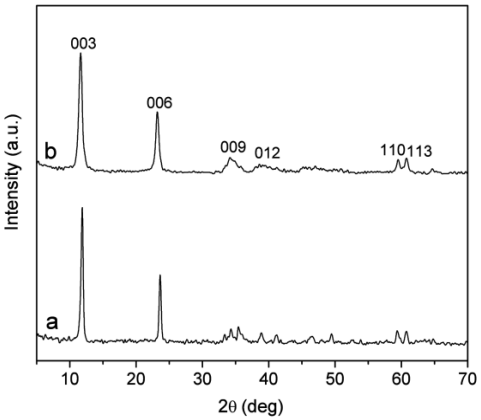

Fig. 1 XRD patterns of (a) CoFe-LDHs and (b) MgCoFe-LDHs.

Dalton Transactions Accepted Manuscript

This journal is © The Royal Society of Chemistry [year]

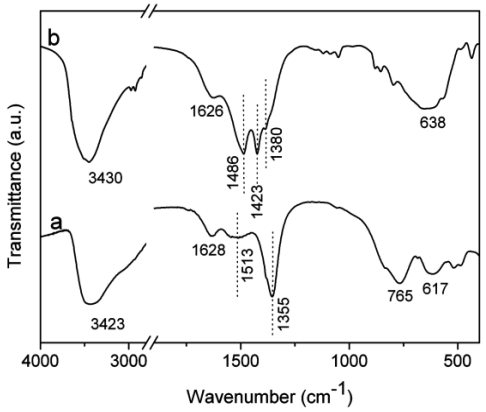

Fig. 2 FT-IR spectra for (a) CoFe-LDHs and (b) MgCoFe-LDHs.

The CoFe-LDHs and MgCoFe-LDHs precursors were synthesized by a method developed in our group involving separate nucleation and aging steps (SNAS method),[10] which facilitates the large-scale synthesis of LDHs nanomaterials. Fig. 1 shows the XRD patterns of the as-synthesized CoFe-LDHs and MgCoFe-LDHs precursors. Evidently, both the two samples display the characteristic diffraction peaks corresponding to the hydrotalcite-like materials, which can be indexed to a hexagonal lattice with $R\bar{3}m$ rhombohedral symmetry.[12] No other crystalline phases were detected, indicating the high purity of the products. The intense and sharp diffraction peaks reveal the good crystallinity and excellently layered feature of the LDHs precursors. The basal (003) spacings are 7.5 Å and 7.8 Å for CoFe-LDHs and MgCoFe-LDHs respectively, indicating the intercalation of CO_3^{2-} species in the interlayer.[13] The average crystallite sizes estimated by the Scherrer's equation are 28.5 nm and 17.4 nm for CoFe-LDHs and MgCoFe-LDHs, respectively.

FT-IR spectra of CoFe-LDHs and MgCoFe-LDHs in the ragion 400-4000 cm^{-1} (Fig. 2) show typical absorption peaks of CO_3^{2-}-intercalated hydrotalcite-like phase.[14] The strong and broad absorption band centered around 3430 cm^{-1} corresponds to the ν (OH) stretching vibrations of hydroxyl groups of brucite-like layers and interlayer water molecules. Another absorption band corresponding to the hydroxyl deformation mode of water (δ H_2O) is recorded at around 1630 cm^{-1}. An intense absorption band at 1355 cm^{-1} can be assigned to the ν_3 symmetry stretching vibrations of carbonate ions. For MgCoFe-LDHs precursor (Fig. 2b), this peak shifts to a higher wavenumber of 1380 cm^{-1}, which can be attributed to the decrease of charge density of the layers, resulting in the weaker interaction between the negatively charged interlayer CO_3^{2-} anions and the positively charged brucite-like layers. Additional bands at 1423/1486/1513 cm^{-1} in the spectra are assigned to the bicarbonate or carbonate ions adsorbed on the external surface of the LDHs crystallites. Other bands observed in the low-frequency region (500 cm^{-1}–800 cm^{-1}) of the spectra are attributed to metal-oxygen and metal-hydroxyl vibrations in the lattice of LDHs.

The thermal behaviors of the as-prepared CoFe-LDHs and MgCoFe-LDHs precursors were studied by TG-DTA analysis as shown in Fig. 3. For the thermal decomposition of the CoFe-LDHs precursor, the weight loss occured essentially in two steps.[8] The first one in the temperature range from room temperature to approximately 200 °C is mainly due to the

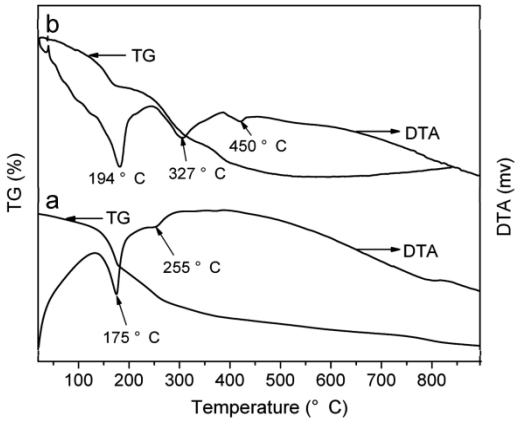

Fig. 3 TG-DTA curves for (a) CoFe-LDHs and (b) MgCoFe-LDHs.

removal of water adsorbed on the external surface of the LDHs as well as water intercalated in the interlayer gallery. The second weight loss involves dehydroxylation of the brucite-like layers and decomposition of the interlayer CO_3^{2-} anions, accompanied by an endothermic event in the DTA at about 255 °C. For MgCoFe-LDHs, the process for weight loss consists of three steps in the TG curve and corresponds to three endothermic events in the DTA curve extending from room temperature to 500 °C, which includes removal of water physisorbed on the external surface and interlayer structure water, dehydroxylation of the layers, and decomposition of the interlayer CO_3^{2-} anions, respectively. All the results indicate that the introduction of Mg atoms onto the LDHs layer increases the thermal stability of the LDHs structure.

Further studies about the thermal decomposition process of CoFe-LDHs and MgCoFe-LDHs precursors were investigated by TPR curves, as shown in Fig. 4. Obviously, the nature of cations has a significant influence on the reducibilities of the LDHs precursors. The weak reduction peaks together with the shoulders in the temperature range 310-430 °C can be attributed to the reduction of Fe^{3+} to its metallic state,[11] accompanied by small amount reduction of Co^{2+} species to metallic Co. Moreover, the peaks do not recover at the baseline, indicating the incomplete reduction of Co^{2+} species.[15a] As reported in the literature,[15b] Co^{2+} in the hydrotalcite exhibits a broad H_2 consumption band from 350 to 700 °C. The broad and strong peak centered at 570 °C corresponds to the complete reduction of Co^{2+} species to their

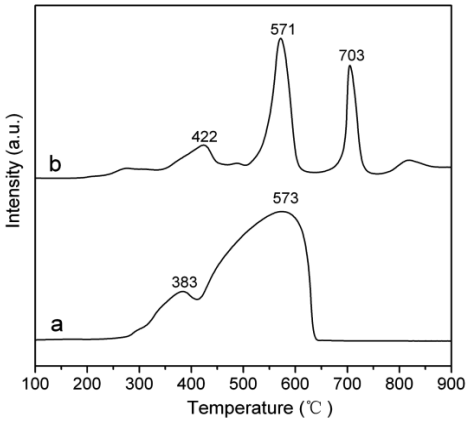

Fig. 4 H_2-TPR curves of (a) CoFe-LDHs and (b) MgCoFe-LDHs.

Dalton Transactions Accepted Manuscript

zerovalent state, resulting in the formation of CoFe alloy. Interestingly, an additional peak at 704 °C was observed in the TPR curve for MgCoFe-LDHs, which can be associated with the reduction of Co^{2+} doped in MgO crystalline lattice to its metallic state Co. This will be discussed in the following XRD analysis.

Synthesis and Characterization of CoFe alloy and CoFe-MgO nanocomposites

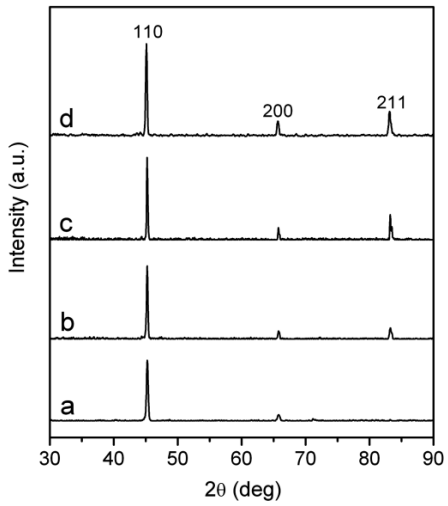

Fig. 5 XRD patterns of samples prepared by reduction of CoFe-LDHs precursor at (a) 450 °C (b) 600 °C (c) 700 °C, and (d) 800 °C.

The crystallite structure of the reduction products obtained from the CoFe-LDHs precursor at different temperatures are investigated by powder XRD patterns as shown in Fig. 5. The corresponding samples are denoted as CF450, CF600, CF700, and CF800 respectively. Evidently, the layered structure of the original LDHs after calcination was completely destroyed and converted into alloy nanoparticles. All the four samples exhibit similar XRD patterns with three diffraction peaks at 2θ = 45.2°, 65.7°, and 83.2°, which are characteristic of the (110), (200), and (211) reflections of a body-centered cubic (bcc) CoFe alloy phase (JCPDS file no. 48-1818). No diffraction peaks belonged to oxide phases (such as CoO, Fe_2O_3) or spinel ($CoFe_2O_4$) phase can be observed, indicating the high purity of the as-prepared CoFe alloy. The intense and sharp diffraction peaks strongly demonstrate the high crystallinity of the products. With the increase of reduction temperature from 450 to 800 °C, the average crystallite size calculated by the Scherrer's equation based on the fwhm of the (110) diffraction peak increases gradually and are 32.4 nm, 45.8 nm, 56.3 nm, and 68.2 nm, respectively.

Fig. 6 shows the SEM images and particle size histograms (inset) of the as-prepared CoFe alloy nanoparticles with different reduction temperatures. Obviously, the diameter of the CoFe alloy particles increases sharply with the increase of reduction temperature, well in accordance with the result of XRD. As we can see from Fig. 6a, CF450 exhibits uniform spherical-like shape with an average particle size of 75 nm. This value is much larger than that calculated by the Scherrer's equation, which can be attributed to the multi-particles aggregation. Furthermore, the as-prepared CoFe alloy particles connect with each other into chain-like particles, which can be attributed to the strong dipole-dipole interaction between individual alloy particles.

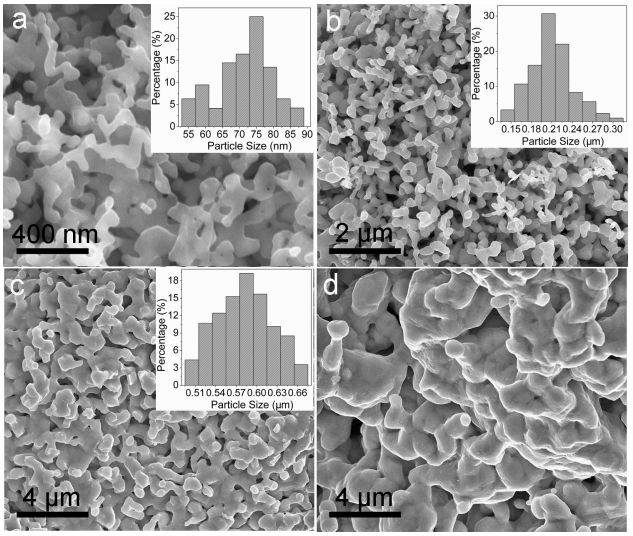

Fig. 6 SEM images and particle size histograms (inset) of samples prepared by reduction of CoFe-LDHs precursor at (a) 450 °C, (b) 600 °C, (c) 700 °C, and (d) 800 °C.

Similar structures were observed for the sample prepared at 600 °C as shown in Fig. 6b, with the average diameter increasing up to 210 nm. With further increase of reduction temperature to 700 °C, the resulting CoFe alloy particles are found to be slightly melted, sintered and agglomerated to large particles with an average size of about 600 nm. For the sample CF800, it was difficult to make out the particles from each other and measure their sizes with high precision, because they have almost lost particulate feature and melted to form a solid solution. The increase of CoFe alloy particles size here is not only affected by the reduction temperatures, but also has close relationship with their soft magnetic behaviour, which has an important influence on the interaction between individual particles.

In the presence of MgO matrix, CoFe-MgO nanocomposites were prepared from the MgCoFe-LDHs precursor. The corresponding products were denoted as MCF450, MCF600, MCF700, and MCF800 respectively. Fig. 7 shows the XRD patterns of the CoFe-MgO nanocomposites prepared at different temperatures. It can be seen that, a cubic MgO phase and bcc

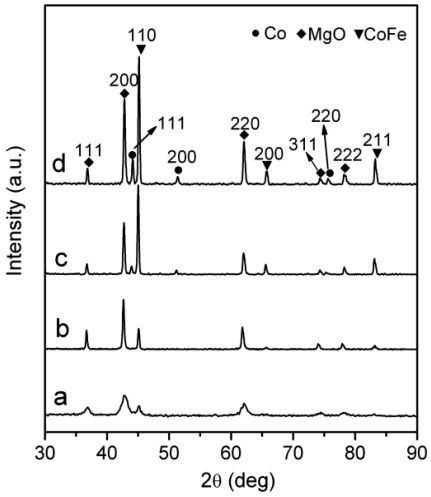

Dalton Transactions Accepted Manuscript

This journal is © The Royal Society of Chemistry [year]

Fig. 7 XRD patterns of samples prepared by reduction of MgCoFe-LDHs precursor at (a) 450 °C (b) 600 °C (c) 700 °C, and (d) 800 °C.

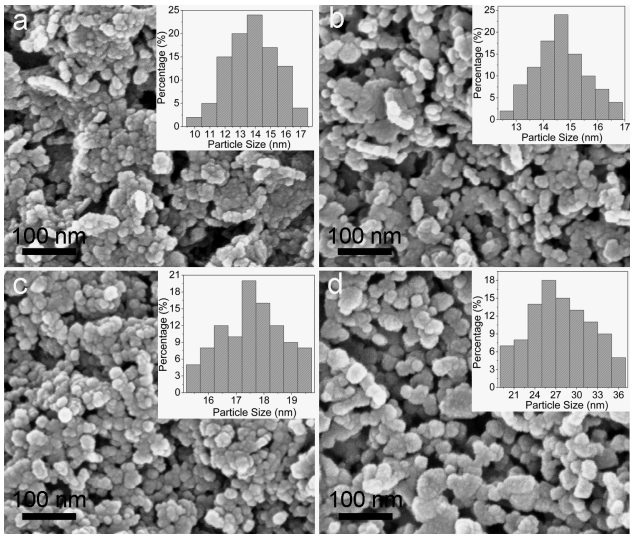

Fig. 8 SEM images and particle size histograms (inset) of samples obtained by reduction of MgCoFe-LDHs precursor at (a) 450 °C (b) 600 °C (c) 700 °C, and (d) 800 °C.

CoFe alloy with good crystallinity are observed in the XRD patterns of all the samples. The five peaks marked (◆) correspond to the (111), (200), (220), (311), and (222) reflections of a cubic MgO phase (JCPDS No. 89-4248) and the peaks marked (▼) are attributed to the (110), (200), (211) reflections of bcc CoFe alloy phase (JCPDS No. 48-1818). Moreover, when the reduction temperature increases up to 700 °C, three additional diffraction peaks are observed at 2θ = 44.17°, 51.46°, and 75.67°, which can be indexed to the (111), (200), and (220) reflections of face-centred cubic (fcc) Co (Fig. 7c). As reported in our previous work,[9] some Co^{2+} and/or partially reduced Fe^{2+} ions have been incorporated in the lattice as a solid solution of MgO with CoO/FeO for sample CF450. In the present study, with the increase of reduction temperature from 450 °C to 800 °C, the lattice parameters of MgO decrease progressively, and are 4.25 Å, 4.24 Å, 4.23 Å and 4.22 Å, respectively, accompanied by the formation of fcc Co phase as shown in Fig. 7. Combined with the result of TPR measurement, we can conclude that some Co^{2+} ions have been incorporated in MgO crystalline lattice at a low reduction temperature and are gradually reduced to its metallic state Co out of the MgO lattice with the increase of calcination temperature, resulting in the formation of pure MgO phase and an additional metallic Co phase.

Fig. 8 shows the SEM images and particle size histograms (inset) of CoFe-MgO nanocomposites to investigate the influence of reduction temperture on the morphology and particle size of the products. As shown in Fig. 8a, sample MCF450 exhibits a platelet-like morphology consisting of spherical shape particles connected with each other, which have an average size of 13.6 nm. Similar structures with some multiparticles aggregates are also observed for MCF600 and the average particle size is about 14.5 nm. Further increase of the reduction temperatures to 700 °C and 800 °C, the platelet-like morphology disappears and the particulate feature becomes more evident with average particle sizes measured to be 17.5 nm and 25.7 nm, respectively. Obviously, there is only a small increase in particle size and no large aggregates or sintering are observed even when the reduction temperature increases up to 800 °C, indicating the high

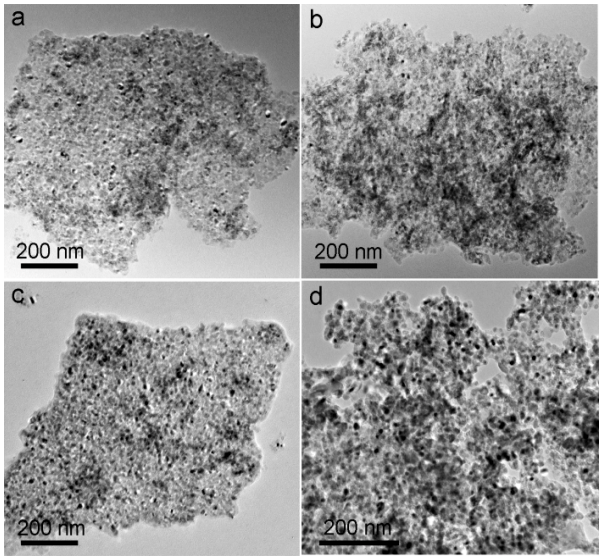

Fig. 9 TEM images of samples prepared by reduction of MgCoFe-LDHs precursor at (a) 450 °C (b) 600 °C (c) 700 °C, and (d) 800 °C.

thermal stability of the as-prepared CoFe-MgO nanocomposites. However, from the SEM images, it is difficult to distinguish CoFe alloy particles and MgO matrix from each other. Further information on the microstructure of the as-prepared CoFe-MgO nanocomposites were investigated by TEM. As shown in Fig. 9, all the samples exhibit similar morphology with uniform CoFe alloy nanoparticles (dark spots) homogeneously dispersed in the MgO matrix (bright region). No aggregation of particles can be observed in the planar view images of all the samples. The average CoFe alloy nanoparticle sizes are calculated to be 8.8 nm, 9.0 nm, 9.4 nm, and 10.5 nm, respectively for MCF450 to MCF800. These values are significantly smaller than that of pure CoFe alloy particles obtained from the CoFe-LDHs precursor, which can be attributed to the pinning effect of surrounding MgO matrix, which can effectively prevent the growth of CoFe alloy particles during the process of thermal decomposition and reduction. The negligible increase of particle size for samples prepared at different temperatures further demonstrated the high thermal stability of the as-obtained nanocomposites. Moreover, it is interesting to find that higher particle density can be observed with the increase of reduction temperature, especially for MCF700 and MCF800 (Fig. 9c and 9d), which is further indicative of the reduction of Co^{2+} doped in MgO crystalline lattice to the fcc Co phase, well in accordance with the TPR and XRD results.

As reported in literature,[4b] the magnetic properties of nanomaterials are probably those which show the most dramatic dependence on composition, particle size and their dispersion. The temperature-dependent magnetization of the resulting CoFe alloy and CoFe-MgO nanocomposites were investigated by vibrating sample magnetometer (VSM) at room temperature. Fig. 10 shows the room temperature magnetization hysteresis loops of the CoFe alloy (Fig. 10a) and CoFe-MgO nanocomposites (Fig. 10b). It can be seen that, all the samples exhibit the typical ferromagnetic bahaviors and the corresponding saturation

Dalton Transactions Accepted Manuscript

magnetization strength (Ms) and coercivity (Hc) values are listed in table 1. The Ms values of CoFe alloy nanoparticles increase with increasing reduction temperature and are 197 emu/g, 202

Table1. Saturation Magnetization (Ms) and Coercivity (Hc) Values of CoFe alloy and CoFe-MgO nanocomposites prepared at different temperatures.

CF/MCF	450 ℃	600 ℃	700 ℃	800 ℃
Ms (emu/g)	197/ 30	202/ 63	209/ 80	213/ 89
Hc (Oe)	296/ 663	227/ 461	177/ 266	190/ 203

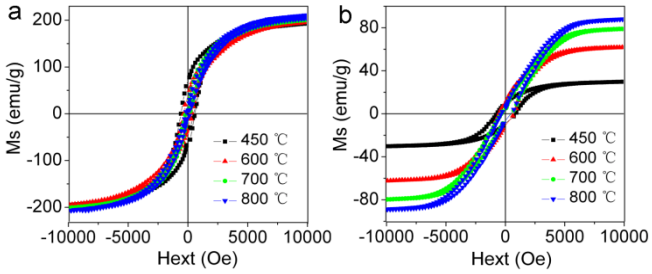

Fig. 10 Room temperature hysteresis loops of (a) CoFe alloy and (b) CoFe-MgO nanocomposites prepared at different temperatures.

emu/g, 209 emu/g, and 213 emu/g, respectively for CF450 to CF800, almost close to that of bulk CoFe alloy (230 emu/g) reported in the literature.[16a] Such high Ms values obtained here can be attributed to the high purity and well crystallinity of the CoFe particles. The coercivities of the CoFe alloy are also much higher than that of bulk CoFe alloy (0.68 Oe or 10-60 Oe).[16b] For CoFe-MgO nanocomposites, as shown in Table 1, relatively smaller Ms values compared to the pure CoFe alloy are obtained from the hysteresis loops, which can be attributed to the relatively small particle size and low loading percentage of the magnetic CoFe alloy in the composites. However, greatly enhanced coercivities are obtained and measured to be 663 Oe, 461 Oe, 266 Oe, and 203 Oe, respectively for MCF450 to MCF80, which are almost 2 orders of magnitude higher than that of bulk CoFe alloy. As demonstrated in our previous work,[9] the enhancement of coercivity can be attributed to the strong surface effects in the very small CoFe particles and the strong interaction between alloy particles and diamagnetic MgO matrix. All the results indicate the excellent magnetic properties of both the CoFe alloy nanoparticles and the CoFe-MgO nanocomposites and their potential applications in magnetic devices. The storage stabilities in air of the CoFe alloy and CoFe/MgO nanocomposites were also tested by XRD and magnetic measurements (not shown here). No significant changes in material compositions and magnetic characteritics were observed after storage in air for 6 months at room temperature, indicating the high air-stability of the as-prepared samples.

Conclusions

In summary, individual CoFe alloy nanoparticles and CoFe-MgO nanocomposites are successfully syntheiszed from layered double hydroxide (LDH) precursors at different temperatures. The as-synthesized CoFe alloy nanoparticles are highly crystalized and the particle size increases sharply from 75 nm to several hundreds nm with the increase of reduction temperature. For CoFe-MgO nanocomposites, CoFe alloy nanoparticles are homogeneously dispersed in the MgO matrix and a narrow particle diameter distribution in the range of 8-11 nm is obtained due to the effective prevention of MgO matrix in the alloy particle growth. Magnetic properties measurement indicate that the as-prepared CoFe alloy particles are excellent soft magnetic materials and the saturation magnetization strength increases from 197 emu/g to 213 emu/g with the increase of reduction temperature, comparable to that of bulk CoFe alloy. In the presence of diamagnetic MgO matrix, the coercivity of the CoFe-MgO nanocomposites is greatly enhanced to 663 Oe due to the strong surface effects in the very small CoFe particles and the strong interaction between alloy particles and the matrix. Both of the as-obtained CoFe alloy and CoFe-MgO nanocomposites exhibit potential applications in magnetic devices.

Acknowledgements

The authors are grateful for financial support from the National Natural Science Foundation of China and the Beijing Natural Science Foundation (2122048).

Author addresses

[a] *State Key Laboratory of Chemical Resource Engineering, Beijing University of Chemical Technology, Beijing, 100029, P. R. China. E-mail: 2011400138@grad.buct.edu.cn; Fax: +86-10-64425385; Tel: +86-10-64451027*

[b] *Environmental Engineering Program, Department of Civil Engineering, Auburn University, Auburn, AL 36849, USA*

References

1 (a) W. W. Pang, S. Lim, Y. Z. Zhang, S. H. Yoon and I. Mochida, *J. Phys. Chem. C.,* 2008, **112**, 10050-10060; (b) I. Robinson, S. Zacchini, L. D. Tung, S. Maenosono and N. T. K. Thanh, *Chem. Mater.*, 2009, **21**, 3021-3026.

2 (a) W. S. Seo, J. H. Lee, X. Sun, Y. Suzuki, D. Mann, Z. Liu, M. Terashima, P. C. Yang, M. V. Mcconnell, S. G. Nishimura and H. Dai, *Nat. Mater.*, 2006, **5**, 971-976; (b) J. Zhang, J. Müller, W. Zheng, D. Wang, D. Su and R. Schlögl, *Nano Lett.*, 2008, **8**, 2738-2743; (c) X. G. Liu, D. Y. Geng and Z. D. Zhang, *Appl. Phys. Lett.*, 2008, **92**, 243110.

3 (a) G. Ennas, A. Falqui, G. Paschina and G. Marongiu, *Chem. Mater.*, 2005, **17**, 6486-6491; (b) N. O. Núñez, P. Tartaj, M. P. Morales, R. Pozas, M. Ocaña and C. J. Serna, *Chem. Mater.*, 2003, **15**, 3558-3563.

4 (a) B. Folch, J. Larionova, Y. Guari, L. Datas and C. Guérin, *J. Mater. Chem.,* 2006, **16**, 4435-4442; (b) G. Ennas, A. Falqui, S. Marras, C. Sangregorio and G. Marongiu, *Chem. Mater.*, 2004, **16**, 5659-5663.

5 (a) M. Mandal, S. Kundu, T. K. Sau, S. M. Yusuf and T. Pal, *Chem. Mater.,* 2003, **15**, 3710-3715; (b) Z. H. Wang, C. J. Choi, J. C. Kim, B. K. Kim and Z. D. Zhang, *Mater. Lett.*, 2003, **57**, 3560-3564; (c) H. M. Song, J. H. Hong, Y. B. Lee, W. S. Kim, Y. Kim, S. J. Kim and N. H. Hur, *Chem. Commun.,* 2006, **6**, 1292-1294.

6 (a) A. Corrias, M. F. Casula, A. Falqui and G. Paschina, *Chem. Mater.*, 2004, **16**, 3130-3138; (b) M. F. Casula, A. Corrias, A. Falqui, V. Serin, D. Gatteschi, C. Sangregorio, C. J. Fernández and G. Battaglin, *Chem. Mater.*, 2003, **15**, 2201-2207.

7 (a) A. Berenbaum, M. Ginzburg-Margau, N. Coombs, A. J. Lough, A. Safa-Sefat, J. E. Greedan, G. A. Ozin and I. Manners, *Adv. Mater.*, 2003, **15**, 51-55; (b) K. Liu, S. B. Clendenning, L. Friebe, W. Y. Chan, X. Zhu, M. R. Freeman, G. C. Yang, C. M. Yip, D. Grozea, Z. H. Lu, I. Manners, *Chem. Mater.*, 2006, **18**, 2591-2601.

Dalton Transactions Accepted Manuscript

This journal is © The Royal Society of Chemistry [year]

8 (a) F. Li, J. Liu, D. G. Evans and X. Duan, *Chem. Mater.,* 2004, **16**,1597-1602; (b) L. Zou, X. Xiang, J. Fan, F. Li, *Chem. Mater.,* 2007**, 19**, 6518-6527; (c) X. Xiang, H. I. Hima, H. Wang and F. Li, *Chem. Mater.,* 2008**, 20**, 1173-1182.

9 L. Wang, J. Liu, Y. Zhou, Y. Song, J. He, D. G. Evans, *Chem. Commun.,* 2010, **46**, 3911-3913.

10 (a) L. Wang, C. Li, M. Liu, D. G. Evans and X. Duan, *Chem. Commun.,* 2007, **2**, 123-125; (b) Y. Zhao, F. Li, R. Zhang, D. G. Evans and X. Duan, *Chem. Mater.,* 2002, **14**, 4286-4291.

11 M. Arco, P. Malet, R. Trujillano and V. Rives, *Chem. Mater.*, 1999, **11**, 624-633.

12 (a) P. J. Sideris, U. G. Nielsen, Z. Gan and C. P. Grey, *Science,* 2008, **321**, 113-117; (b) X. Zhao, F. Zhang, S. Xu, D. G. Evans and X. Duan, *Chem. Mater.,* 2010**, 22**, 3933-3942.

13 (a) Y. Han, Z. H. Liu, Z. Yang, Z. Wang, X. Tang, T. Wang, L. Fan and K. Ooi, *Chem. Mater.*, 2008, **20**, 360-363; (b) Z. P. Xu and G. Q. Lu, *Chem. Mater.*, 2005, **17**, 1055-1062.

14 (a) H. Chen, F. Zhang, S. Fu and X. Duan, *Adv. Mater*., 2006, **18**, 3089-3093; (b) N. Iyi, T. Matsumoto, Y. Kaneko and K. Kitamura, *Chem. Mater.*, 2004, **16**, 2926-2932.

15 (a) S. Velu, K. Suzuki, M. P. Kapoor, S. Tomura, F. Ohashi and T. Osaki, *Chem. Mater.*, 2000, **12**, 719-730; (b) S. Velu, K. Suzuki, s. Hashimoto, N. Satoh, F. Ohashi and S. Tomura, *J. Mater. Chem.,* 2001, **11**, 2049-2060.

16 (a) C. W. Kim, Y. H. Kim, H. G. Cha, H. W. Kwon and Y. S. Kang, *J. Phys. Chem. B,* 2006, **110**, 24418-24423; (b) X. W. Wei, G. X. Zhu, Y. J. Liu, Y. H. Ni, Y. Song and Z. Xu, *Chem. Mater*., 2008, **20**, 6248-6253.

Dalton Transactions Accepted Manuscript

Graphical Abstract

Individual CoFe alloy nanoparticles and CoFe-MgO nanocomposites were prepared by the thermal reduction of single-source layered double hydroxides (LDHs) precursors at different temperatures. The reduction temperature has a significant influence on the composition, particle size and size distribution, as well as the magnetic properties of the resulting materials. Magnetic measurement indicates that the as-obtained CoFe alloy nanoparticles and CoFe-MgO nanocomposites exhibit excellent magnetic properties with extremely high Ms value (213 emu/g) and greatly enhanced coercivity (663 Oe), respectively, implying their potential applications in data storage and other magnetic devices.

Cover Picture

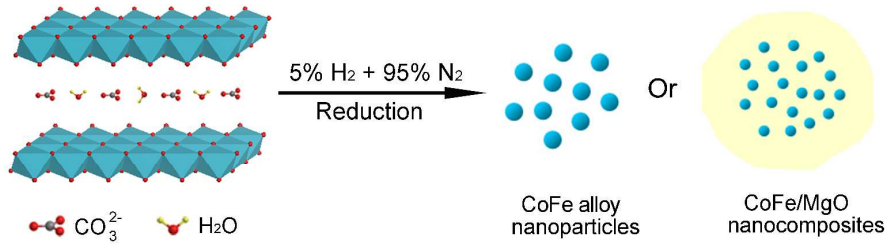

Dalton Transactions Accepted Manuscript